An Hybrid Multi-Task Bayesian Compressive Born Iterative Microwave Imaging Approach

G. Oliveri, L. Poli, N. Anselmi, M. Salucci, and A. Massa

Abstract

This work presents an innovative microwave imaging method to retrieve non-weak targets in the compressive sensing (*CS*) framework. In order to avoid the contrast source formulation (*CSF*) of the arising inverse scattering (*IS*) problem, a Born Iterative (*BI*) formulation is adopted, and the estimation of the unknown contrast function within the imaged domain is carried out by means of an iterative approach thanks to a customized multi-task Bayesian compressive sensing (*MT-BCS*) method. Some preliminary results are reported in order to verify the effectiveness of the proposed hybrid *BI-MT-BCS* solution strategy, as well as to highlight its current limitations.

Contents

1 Numerical Assessment

1.1 Square-shaped Object, $\ell = \lambda/3$

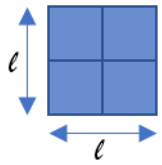

Figure 1: Square-shaped Object

Test Case Description

Direct solver:

- Cubic domain divided in $\sqrt{D} \times \sqrt{D}$ cells
- Number of cells for the direct solver: $D = 1296$ (discretization $= \lambda/12$)

Inverse solver:

- Cubic domain divided in $\sqrt{N} \times \sqrt{N}$ cells
- Number of cells for the inversion: $N = 324$ (discretization $= \lambda/6$)

Measurement domain:

- Total number of measurements: $M = 27$
- Measurement points placed on circles of radius $\rho = 3\lambda$

Sources:

- Plane waves
- Number of views: $V = 4$; $\theta_{inc}^{v} = 0° + (v-1) \times (360/V)$
- Amplitude: $A = 1.0$
- Frequency: $F = 300$ MHz ($\lambda = 1$)

Background:

- $\varepsilon_r = 1.0$
- $\sigma = 0$ [S/m]

Scatterer

- Square-shaped object, $\ell = \lambda/3$
- $\varepsilon_r \in 3.0$
- $\sigma = 0$ [S/m]

Born Iterative Method

- $I_{MAX} = 10$
- $\eta = 10^{-3}$

1.1.1 Square-shaped Object, $\ell = \lambda/3$ - MT-BCS reconstructed profiles with first Born approximation

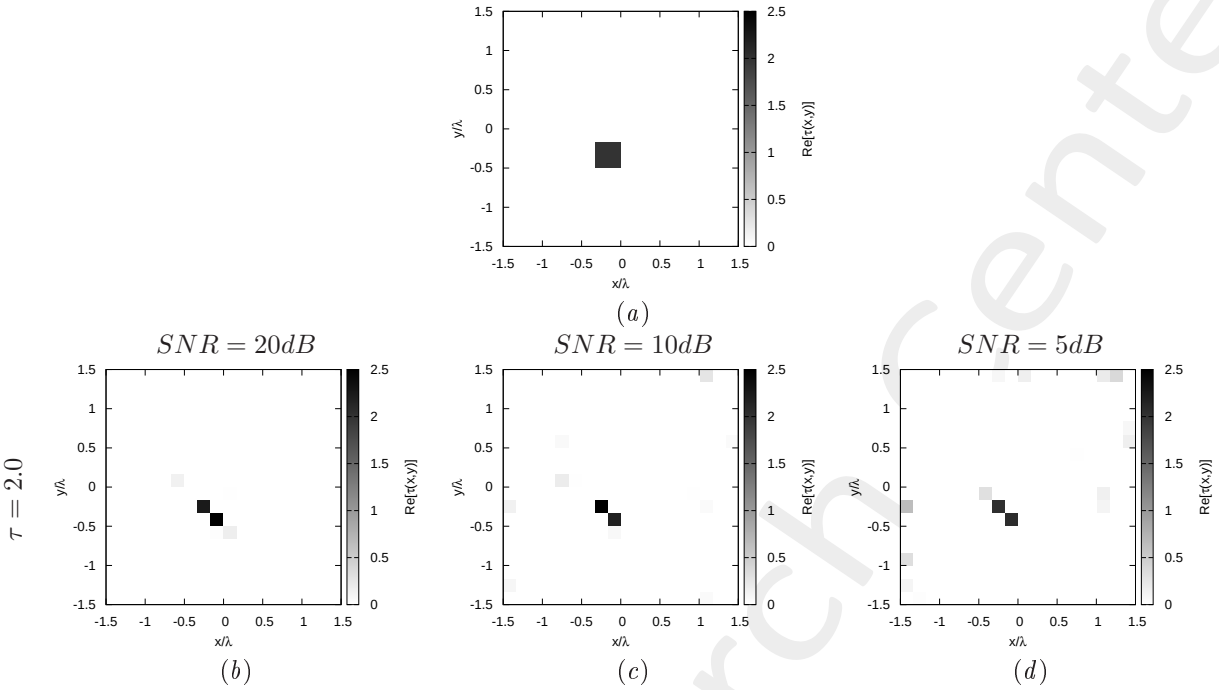

Figure 2: *Square-shaped Object,* $\ell = \lambda/3$: (a) Direct problem with $\tau = 2.0$, (b) MT-BCS reconstructed profiles for $SNR = 20$ [dB], (c) $SNR = 10$ [dB] and (d) $SNR = 5$ [dB]

1.1.2 Square-shaped Object, $\ell = \lambda/3$ - MT-BCS reconstructed profiles with Born Iterative Method ($I_{MAX} = 10$)

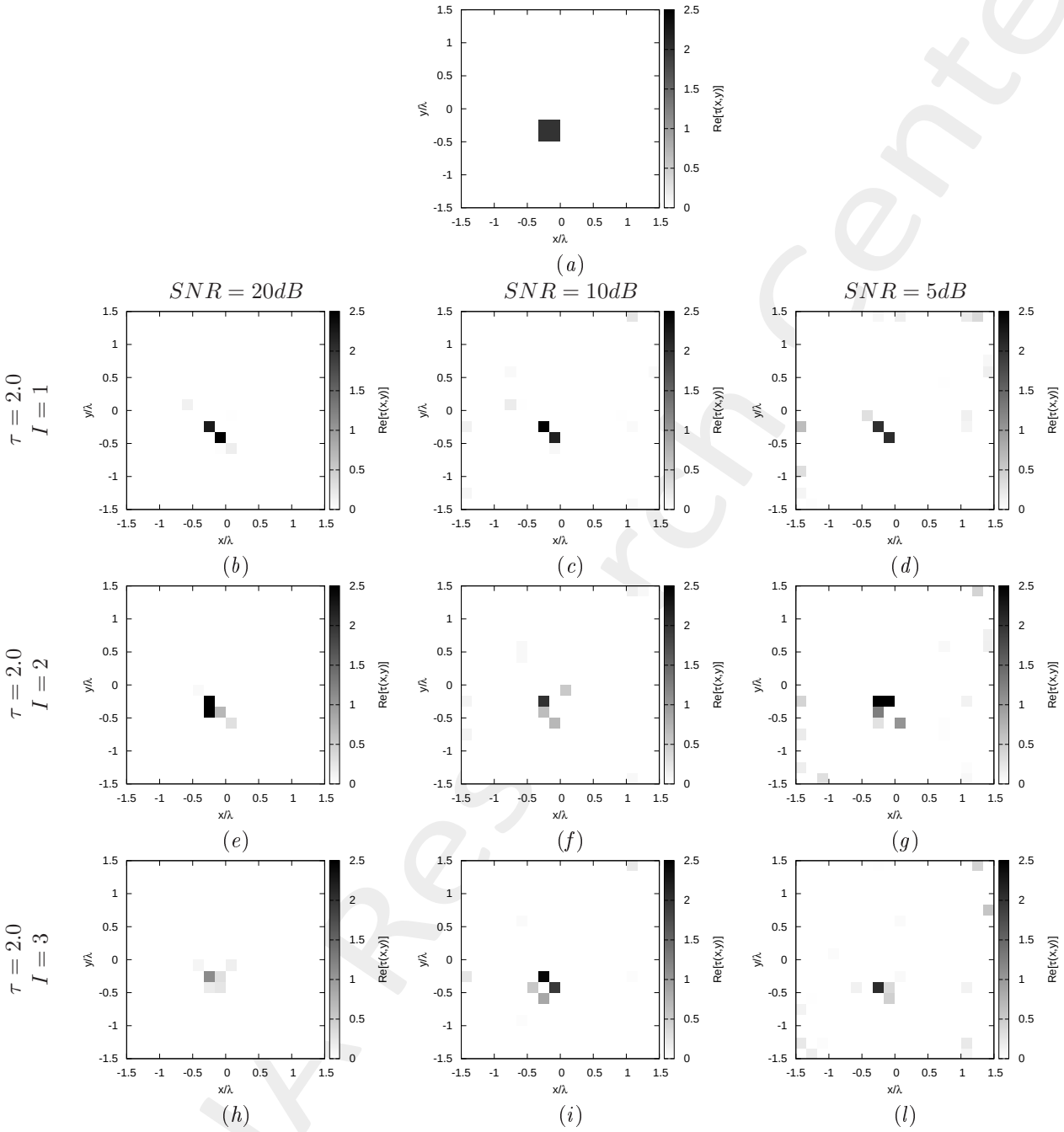

Figure 3: *Square-shaped Object,* $\ell = \lambda/3$: (a) Direct problem with $\tau = 2.0$, $(b)(e)(h)$ MT-BCS reconstructed profiles for $SNR = 20$ [dB], $(c)(f)(i)$ $SNR = 10$ [dB] and $(d)(g)(l)$ $SNR = 5$ [dB] with (b)-(d) Born Iterative Method at the first iteration ($I = 1$), (e)-(g) Born Iterative Method at the second iteration ($I = 2$), (h)-(l) Born Iterative Method at the third iteration ($I = 3$)

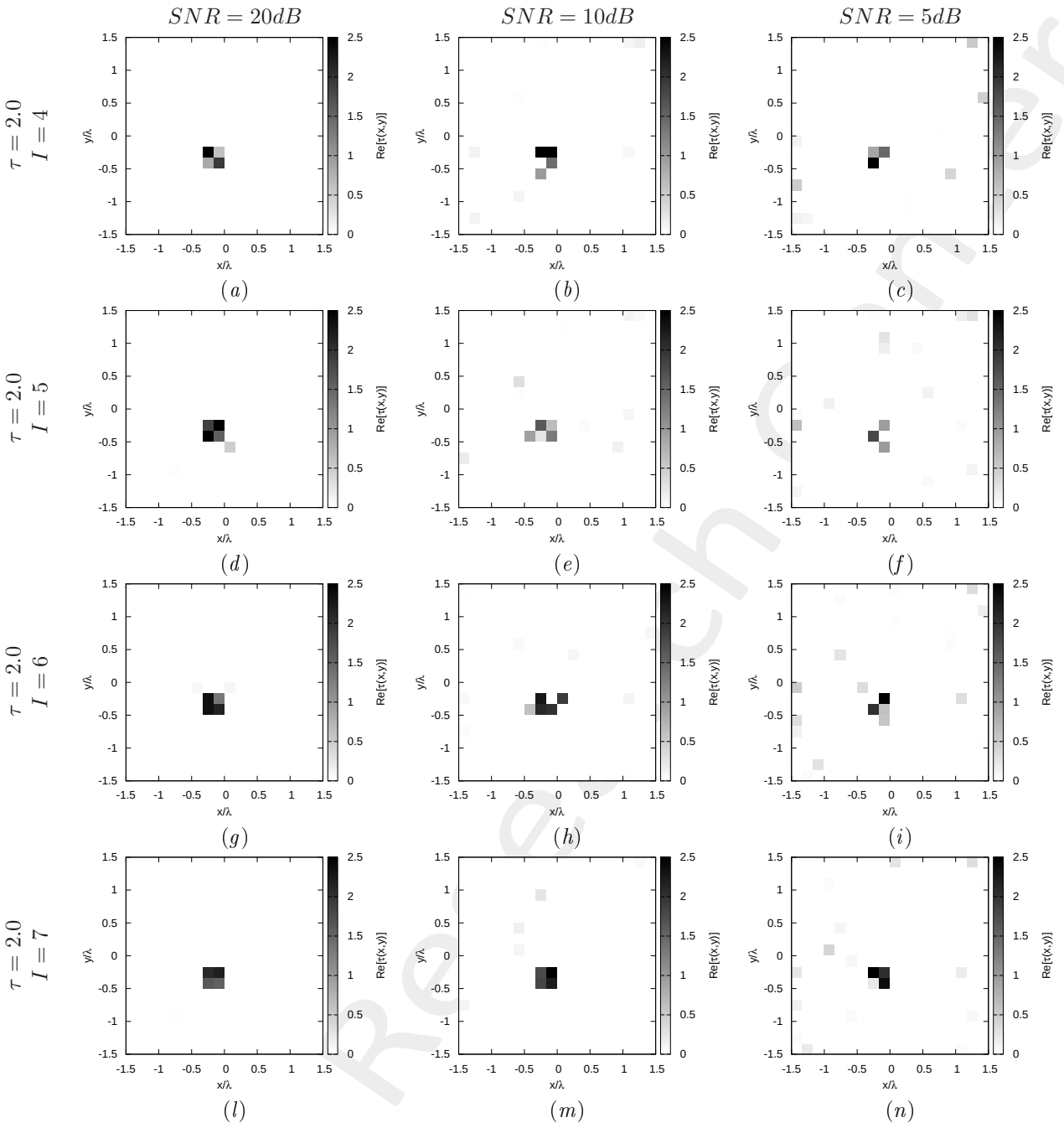

Figure 4: *Square-shaped Object,* $\ell = \lambda/3$: $(a)(d)(g)(l)$ MT-BCS reconstructed profiles for $SNR = 20$ [dB], $(b)(e)(h)(m)$ $SNR = 10$ [dB] and $(c)(f)(i)(n)$ $SNR = 5$ [dB] with (a)-(c) Born Iterative Method at the fourth iteration ($I = 4$), (d)-(f) Born Iterative Method at the fifth iteration ($I = 5$), (g)-(i) Born Iterative Method at the sixth iteration ($I = 6$) , (l)-(n) Born Iterative Method at the seventh iteration ($I = 7$)

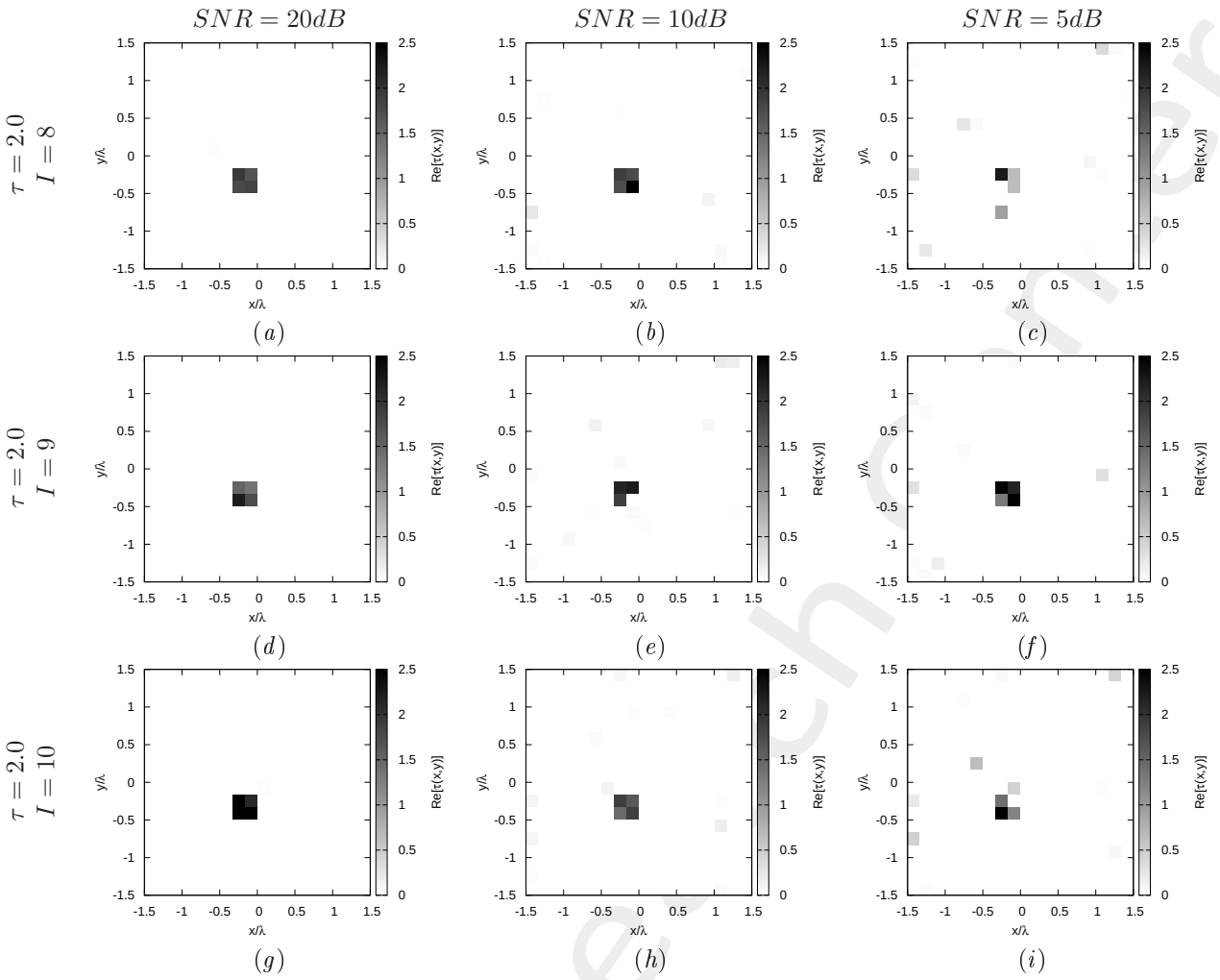

Figure 5: *Square-shaped Object,* $\ell = \lambda/3$: $(a)(d)(g)(l)$ MT-BCS reconstructed profiles for $SNR = 20$ [dB], $(b)(e)(h)(m)$ $SNR = 10$ [dB] and $(c)(f)(i)(n)$ $SNR = 5$ [dB] with (a)-(c) Born Iterative Method at the eighth iteration ($I = 8$), (d)-(f) Born Iterative Method at the ninth iteration ($I = 9$), (g)-(i) Born Iterative Method at the tenth iteration ($I = 10$)

1.1.3 Square-shaped Object, $\ell = \lambda/3$ - MT-BCS reconstructed profiles with Born Iterative Method (Threshold η)

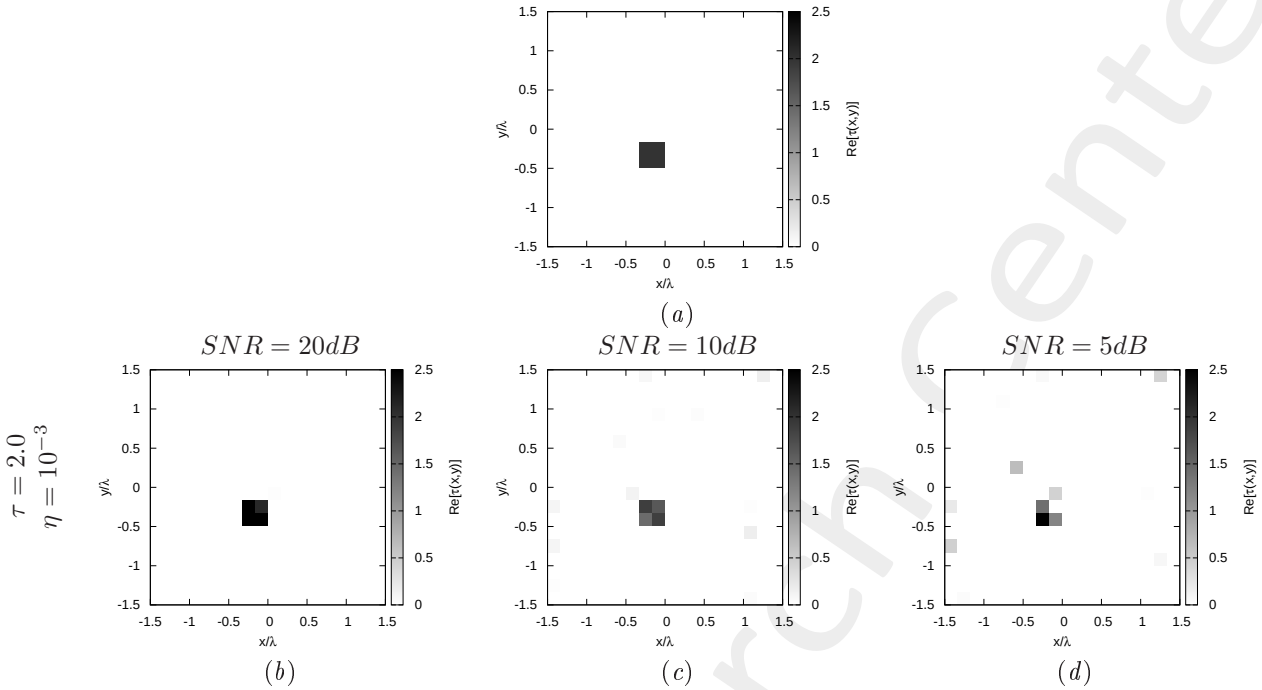

Figure 6: *Square-shaped Object,* $\ell = \lambda/3$: (a) Direct problem with $\tau = 2.0$, (b) MT-BCS reconstructed profiles for $SNR = 20$ [dB], (c) $SNR = 10$ [dB] and (d) $SNR = 5$ [dB] with (b)-(d) Born Iterative Method with threshold $\eta = 10^{-3}$

1.2 L-shaped Object, $\ell = \lambda/2$

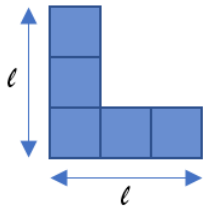

Figure 7: L-shaped Object

Test Case Description

Direct solver:

- Cubic domain divided in $\sqrt{D} \times \sqrt{D}$ cells
- Number of cells for the direct solver: $D = 1296$ (discretization $= \lambda/12$)

Inverse solver:

- Cubic domain divided in $\sqrt{N} \times \sqrt{N}$ cells
- Number of cells for the inversion: $N = 324$ (discretization $= \lambda/6$)

Measurement domain:

- Total number of measurements: $M = 27$
- Measurement points placed on circles of radius $\rho = 3\lambda$

Sources:

- Plane waves
- Number of views: $V = 4$; $\theta_{inc}^{v} = 0^{\circ} + (v-1) \times (360/V)$
- Amplitude: $A = 1.0$
- Frequency: $F = 300$ MHz ($\lambda = 1$)

Background:

- $\varepsilon_r = 1.0$
- $\sigma = 0$ [S/m]

Scatterer

- L-shaped object, $\ell = \lambda/2$
- $\varepsilon_r \in \{1.5, 2.0, 3.0\}$
- $\sigma = 0$ [S/m]

Born Iterative Method

- $I_{MAX} = 10$
- $\eta = 10^{-3}$

1.2.1 L-shaped Object, $\ell = \lambda/2$ - $\tau = 0.5$

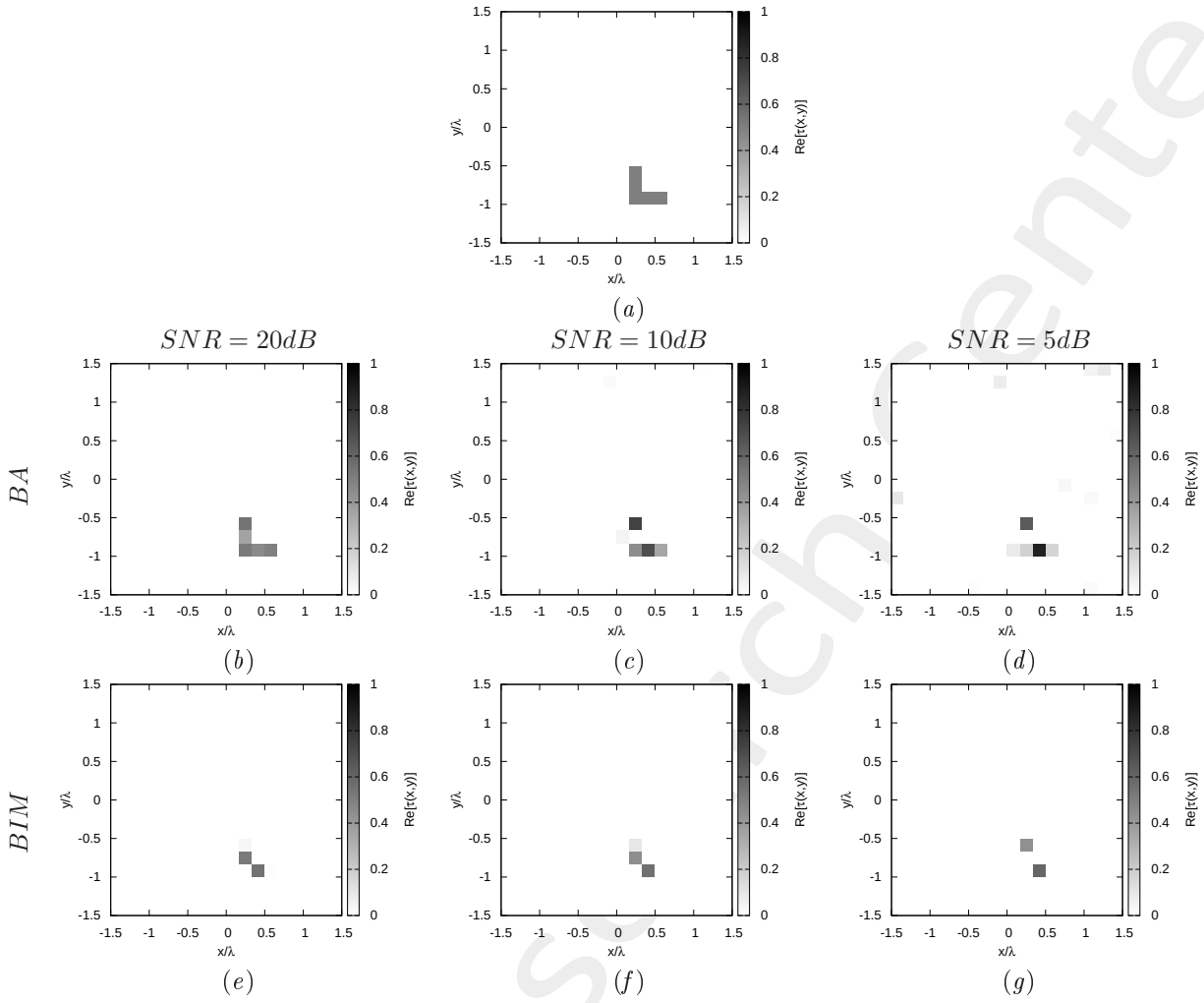

Figure 8: *L-shaped Object,* $\ell = \lambda/2$: (a) Direct problem with $\tau = 0.5$, $(b)(e)$ MT-BCS reconstructed profiles for $SNR = 20$ [dB], $(c)(f)$ $SNR = 10$ [dB] and $(d)(g)$ $SNR = 5$ [dB] with (b)-(d) First Born approximation, (e)-(g) Born Iterative Method

1.2.2 L-shaped Object, $\ell = \lambda/2$ - $\tau = 1.0$

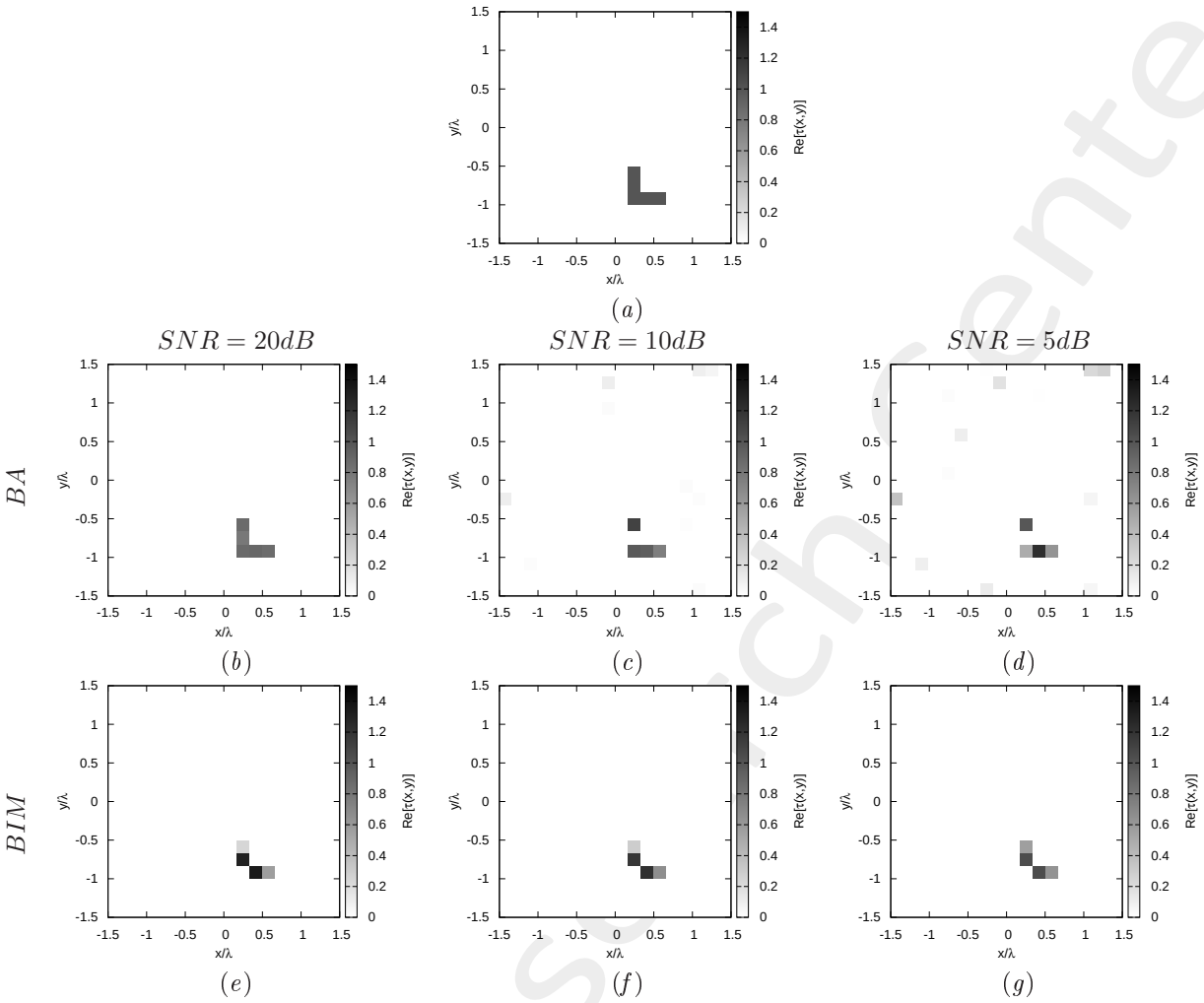

Figure 9: *L-shaped Object,* $\ell = \lambda/2$: (a) Direct problem with $\tau = 1.0$, $(b)(e)$ MT-BCS reconstructed profiles for $SNR = 20$ [dB], $(c)(f)$ $SNR = 10$ [dB] and $(d)(g)$ $SNR = 5$ [dB] with (b)-(d) First Born approximation, (e)-(g) Born Iterative Method

1.2.3 L-shaped Object, $\ell = \lambda/2$ - $\tau = 2.0$

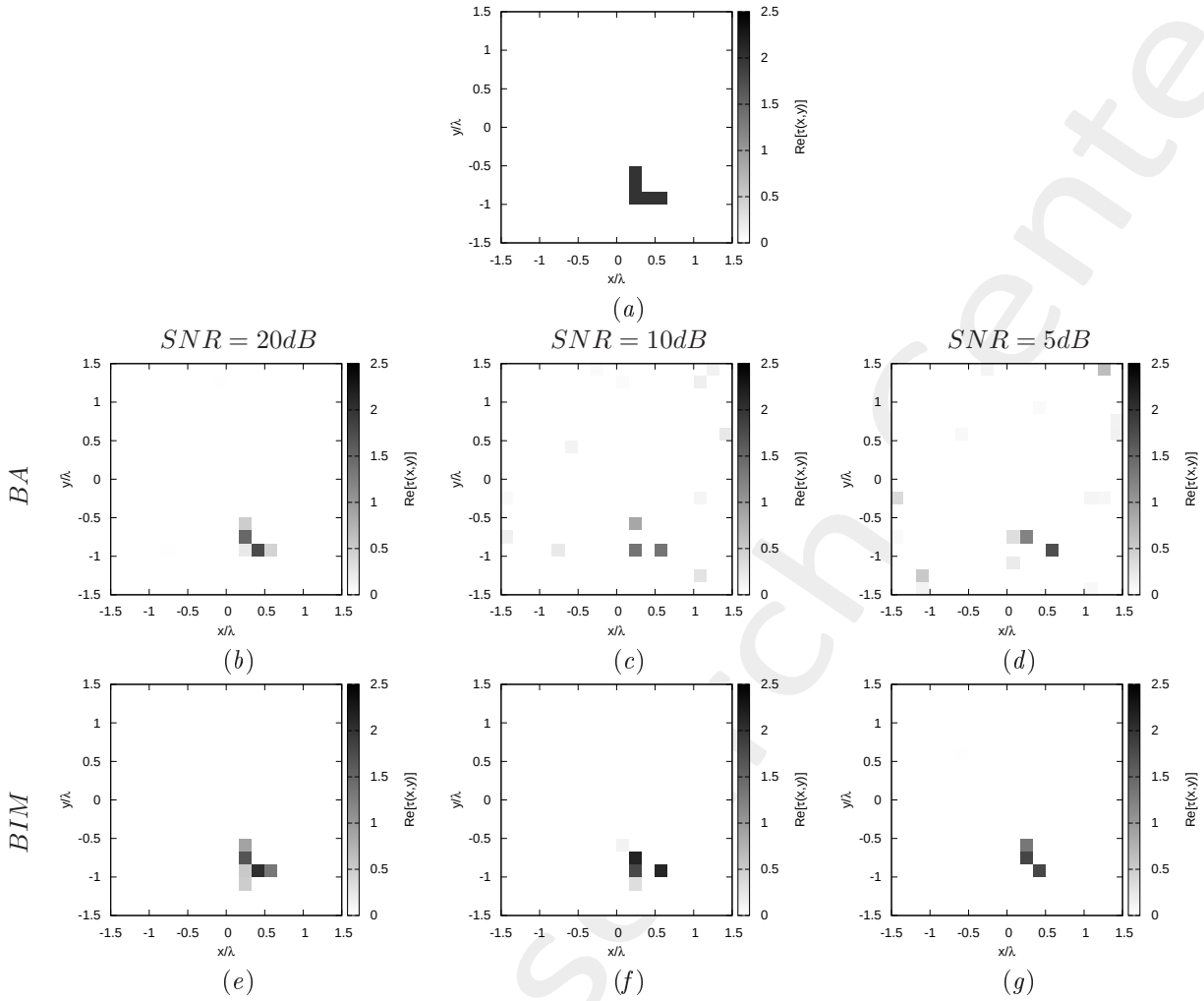

Figure 10: *L-shaped Object*, $\ell = \lambda/2$: (a) Direct problem with $\tau = 2.0$, $(b)(e)$ MT-BCS reconstructed profiles for $SNR = 20$ [dB], $(c)(f)$ $SNR = 10$ [dB] and $(d)(g)$ $SNR = 5$ [dB] with (b)-(d) First Born approximation, (e)-(g) Born Iterative Method

References

[1] G. Oliveri, M. Salucci, N. Anselmi, and A. Massa, "Compressive sensing as applied to inverse problems for imaging: theory, applications, current trends, and open challenges," *IEEE Antennas Propag. Mag.*, vol. 59, no. 5, pp. 34-46, Oct. 2017.

[2] A. Massa, P. Rocca, and G. Oliveri, "Compressive sensing in electromagnetics - A review," *IEEE Antennas Propag. Mag.*, pp. 224-238, vol. 57, no. 1, Feb. 2015.

[3] G. Oliveri, L. Poli, N. Anselmi, M. Salucci, and A. Massa, "Compressive sensing-based Born iterative method for tomographic imaging," *IEEE Trans. Microw. Theory Techn.*, vol. 67, no. 5, pp. 1753-1765, May 2019.

[4] M. Salucci, A. Gelmini, L. Poli, G. Oliveri, and A. Massa, "Progressive compressive sensing for exploiting frequency-diversity in GPR imaging," *Journal of Electromagnetic Waves and Applications*, vol. 32, no. 9, pp. 1164-1193, 2018.

[5] N. Anselmi, L. Poli, G. Oliveri, and A. Massa, "Iterative multi-resolution bayesian CS for microwave imaging," *IEEE Trans. Antennas Propag.*, vol. 66, no. 7, pp. 3665-3677, Jul. 2018.

[6] N. Anselmi, G. Oliveri, M. A. Hannan, M. Salucci, and A. Massa, "Color compressive sensing imaging of arbitrary-shaped scatterers," *IEEE Trans. Microw. Theory Techn.*, vol. 65, no. 6, pp. 1986-1999, Jun. 2017.

[7] N. Anselmi, G. Oliveri, M. Salucci, and A. Massa, "Wavelet-based compressive imaging of sparse targets," *IEEE Trans. Antennas Propag.*, vol. 63, no. 11, pp. 4889-4900, Nov. 2015.

[8] G. Oliveri, N. Anselmi, and A. Massa, "Compressive sensing imaging of non-sparse 2D scatterers by a total-variation approach within the Born approximation," *IEEE Trans. Antennas Propag.*, vol. 62, no. 10, pp. 5157-5170, Oct. 2014.

[9] L. Poli, G. Oliveri, and A. Massa, "Imaging sparse metallic cylinders through a local shape function Bayesian compressive sensing approach," *Journal of Optical Society of America A*, vol. 30, no. 6, pp. 1261-1272, 2013.

[10] L. Poli, G. Oliveri, F. Viani, and A. Massa, "MT-BCS-based microwave imaging approach through minimum-norm current expansion," *IEEE Trans. Antennas Propag.*, vol. 61, no. 9, pp. 4722-4732, Sep. 2013.

[11] L. Poli, G. Oliveri, P. Rocca, and A. Massa, "Bayesian compressive sensing approaches for the reconstruction of two-dimensional sparse scatterers under TE illumination," *IEEE Trans. Geosci. Remote Sens.*, vol. 51, no. 5, pp. 2920-2936, May 2013.

[12] L. Poli, G. Oliveri, and A. Massa, "Microwave imaging within the first-order Born approximation by means of the contrast-field Bayesian compressive sensing," *IEEE Trans. Antennas Propag.*, vol. 60, no. 6, pp. 2865-2879, Jun. 2012.

[13] G. Oliveri, L. Poli, P. Rocca, and A. Massa, "Bayesian compressive optical imaging within the Rytov approximation," *Optics Letters*, vol. 37, no. 10, pp. 1760-1762, 2012.

[14] G. Oliveri, P. Rocca, and A. Massa, "A Bayesian compressive sampling-based inversion for imaging sparse scatterers," *IEEE Trans. Geosci. Remote Sens.*, vol. 49, no. 10, pp. 3993-4006, Oct. 2011.

[15] M. Salucci, A. Gelmini, G. Oliveri, and A. Massa, "Planar arrays diagnosis by means of an advanced Bayesian compressive processing," *IEEE Trans. Antennas Propag.*, vol. 66, no. 11, pp. 5892-5906, Nov. 2018.

[16] L. Poli, G. Oliveri, P. Rocca, M. Salucci, and A. Massa, "Long-distance WPT unconventional arrays synthesis," *Journal of Electromagnetic Waves and Applications*, vol. 31, no. 14, pp. 1399-1420, Jul. 2017.

[17] G. Oliveri, M. Salucci, and A. Massa, "Synthesis of modular contiguously clustered linear arrays through a sparseness-regularized solver," *IEEE Trans. Antennas Propag.*, vol. 64, no. 10, pp. 4277-4287, Oct. 2016.

[18] P. Rocca, M. A. Hannan, M. Salucci, and A. Massa, "Single-snapshot DoA estimation in array antennas with mutual coupling through a multi-scaling BCS strategy," *IEEE Trans. Antennas Propag.*, vol. 65, no. 6, pp. 3203-3213, Jun. 2017.

[19] M. Salucci, L. Poli, and G. Oliveri, "Full-vectorial 3D microwave imaging of sparse scatterers through a multi-task Bayesian compressive sensing approach," *Journal of Imaging*, vol. 5, no. 1, pp. 1-24, Jan. 2019 (DOI: 10.3390/jimaging5010019).